Desalination and Water Treatment
www.deswater.com

10 (2009) 238–244

Heat and mass transfer in a horizontal pipe absorber for a heat transformer

D. Juárez-Romero[a*], N. Shah[b], F. Pliego-Solórzano[a], J.A. Hernández[a], J. Siqueiros[a], A. Huicochea[a]

[a]*Centro de Investigación en Ingeniería y Ciencias Aplicadas (CIICAp), Universidad Autónoma del Estado de Morelos (UAEM), Av. Universidad 1001, Col. Chamilpa, C.P. 62210, Cuernavaca, Morelos, México*
Tel. +52 (777) 329-79-84; Fax +52 (777) 329-79-84; email: djuarezr7@gmail.com
[b]*Process Systems Engineering Imperial College of Science Technology and Medicine, Centre for Process Systems Engineering, South Kensington Campus, Roderick Hill Building, London SW7 2AZ, UK*

Received 30 September 2008; Accepted in revised form October 8, 2009

ABSTRACT

A dynamic model is developed which describes the heat and mass transfer of a horizontal pipe absorber applied to a heat transformer used to purify water. A specific configuration of the pipes is used to evaporate water. This absorber operates with a mixture of LiBr-H_2O, which is distributed from the top and it descends by gravity through the horizontal pipe manifold, passing from one pipe to another. This dynamic model considers three flow regimes: descendant film over each pipe of the refrigerant fluid, a drop formation regime under each pipe, and a free descendant drop from one pipe to the one below. The mathematical model is based in the mass and energy balances, with empirical heat transfer coefficients. With this model, we can identify the relevance of each flow regime. This model represents a useful tool to study the effect of different operating conditions of the absorption heat transformer.

Keywords: Heat transformer; Absorption system; Lithium bromide

1. Introduction

An important energy cycle for heat recovery is the heat transformer, which increases the available heat level to a higher temperature level. In recent years, the absorption heat transformers have drawn the attention as an alternative to the compression heat pumps.

Among the absorption heat transformers, the absorber is a critical component, since its efficiency directly affects the whole cycle. Its advantage is that it does not have moving parts and can operate at low temperatures. Its disadvantage is its associated cost, which is higher due to its large size in comparison with the compression systems. The absorption systems also present slower dynamics. Additionally, these systems work with an absorbent mixture of LiBr-H_2O, which requires corrosion resistant materials. As a result, it is convenient to do a detailed analysis of the absorber. Therefore, to promote the use of this type of heat transformers, dynamic simulation is proposed as a training tool for the operation without the related costs.

Kirby and Pérez-Blanco [1] presented a numerical model with three flow regimes when the absorbent mixture travels from one pipe to another: drop formation at the tube, free droplet fall at the bottom of the tube, and falling film between tubes. Determan [2] comments that in a review carried out by Killion and Garimella [3] film hydrodynamics are not considered. In most models the

* Corresponding author.

Presented at EuroMed 2008, Desalination for Clean Water and Energy Cooperation among Mediterranean Countries of Europe and the MENA Region, 9–13 November 2008, King Hussein Bin Talal Convention Center, Dead Sea, Jordan.

presence of wavy films is usually ignored; absorption in the drop formation regime is not considered; surface wetting effects are seldom accounted for; and experimental validation of models is limited. Kyung et al. [4,5] highlighted the importance of drop formation in the prediction of the absorber performance.

The distinct objective of the present work is to formulate a model, which appropriately describes the phenomena involved when an absorption heat transformer is used to evaporate water. Then, it is possible to compare the dynamic simulation results with the experimental results. Also, to estimate the energy and mass transfer coefficients, with the final aim of evaluating the relevance of each flow regime. This computational model is applied to an experimental model developed at the Center of Research on Engineering and Applied Sciences at the State University of Morelos. This piece of equipment is a component of a portable heat transformer used to purify water by energy-recycle [6]. LiBr-H_2O is used as an absorbent mixture, while water is used as refrigerant flow. Its design characteristics are available, as well as the operating conditions.

2. Experimental description

The absorber is built as a horizontal shell and pipes heater. As water flows through the pipe, the absorbent mixture LiBr-H_2O descends by gravity along the shell. Steam coming from the evaporator ascends in cross current. Then, the components of both streams have an intimate contact promoting mass and energy transfer from the steam to the absorbent mixture. Absorption process releases heat, without modifying the chemical species. This heat is transferred to the refrigerant liquid by crosscurrent.

The dimensions of the experimental equipment are shown in Table 1. To maintain an even flow, in the upper part of the absorber lays a distributor. The pipe manifold receives flow from this distributor. The pipes have lids at both ends. These lids have divisions to promote circulation in four stages along the absorber cylindrical body. The configuration of streams, as described in Fig. 1, is designed to promote a high temperature for the purified stream.

Table 1
Geometric configuration of the absorber [7]

Absorber configuration	Horizontal tube bank in counter flow
Shell	Tube size: 102 mm internal diameter
	Tube length: 400 mm
Array of pipes	
Number of horizontal sections	4; 4–6 pipes per row
Number of pipes	16
Pipe diameter	3/8 in stainless steel 316L, roughed
Pipe pitch	Vertical pitch, triangular: 5mm

3. Absorber mathematical model

To develop the differential equations, which describe the absorber dynamic behavior (see Fig. 2), the model is based in the following assumptions and restrictions:

- Liquid and vapor reach equilibrium at the interphase.
- The physical properties of the absorbent mixture depend on (T, x) at every time step.
- There are not incondensable gases in the steam.
- Inside the absorber, the pressure drop is neglected
- Flows are considered laminar-Newtonian.
- Transfer coefficients are considered empirical and

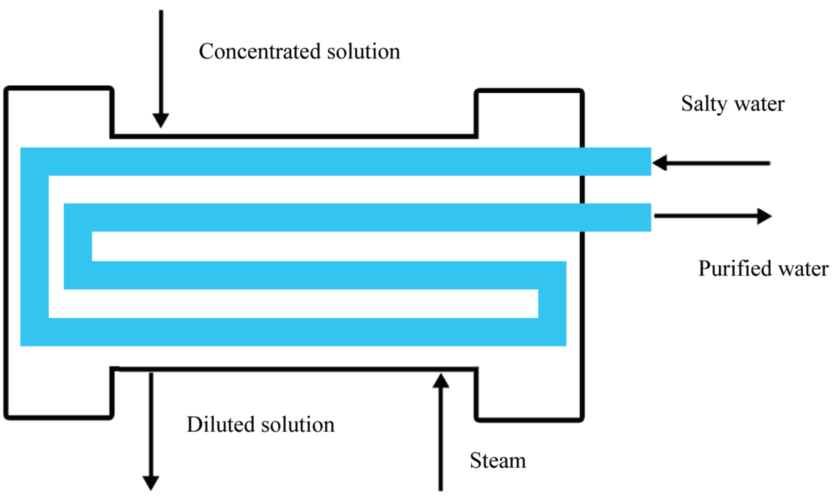

Fig. 1. Equipment configuration of the absorber.

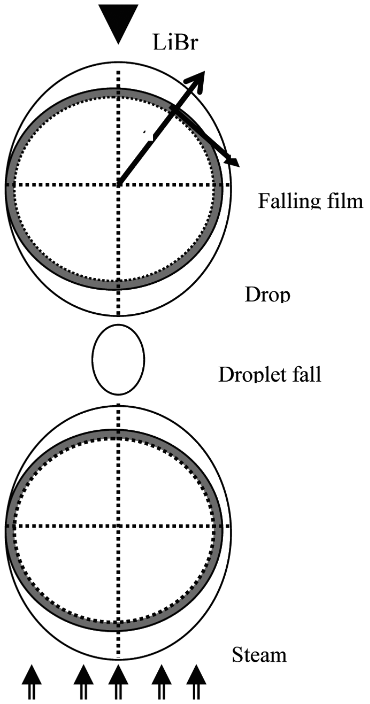

Fig. 2. Flow regimes by pipe.

distinct for every regime.

- Heat transfer from absorbent mixture to steam is negligible.
- The absorbent mixture completely covers the pipe surface
- A bidimensional approximation describes the phenomenon.

3.1. Physical properties

Enthalpy and density were obtained from the correlations developed by Torres-Merino [8], which are based on the work of McNeely [9]. The interphase composition is obtained by Eq. (1):

$$x_i = f\left(T_i, P_V\right) \tag{1}$$

Vapor pressure, P_V is obtained from correlations provided by Poling et al. [10].

3.2. Description of every regime

The equations, which describe the process dynamics, were obtained from mass and energy balances. Kirby and Pérez-Blanco [1] proposed three regimes: drop formation, droplet fall, and falling film. The equations were also obtained from the work of Jeong and Garimella [11].

3.3. Drop formation regime

This regime occurs in the lower part of the refrigerant pipe: since the drop formation begins, and until the formation ends (Fig. 3). Then it drops from the surface to travel to the next pipe.

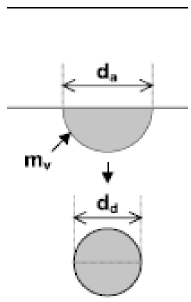

Fig. 3. Drop formation and droplet fall regimes.

In the drop formation regime, the mass and energy equations are the result of a balance in a fine spherical film around the pipe [1,4].

Mass balance

$$\frac{\mathrm{d}m_d}{\mathrm{d}t} = 4K_{\text{form}}\rho\pi R^2 \frac{\left(x_s - x_i\right)}{100} \tag{2}$$

Energy balance

$$m_d Cp_s \frac{\mathrm{d}T_s}{\mathrm{d}t} = h_{abs}\frac{\mathrm{d}m_d}{\mathrm{d}t} + Q \tag{3}$$

The energy balance considers the absorption heat (h_{abs}), and the heat transferred from the center of the newly formed drop to the newly formed fine spherical film (Q).

$$Q = 4K\pi r_d^{\,2}\frac{(T_b - T_i)}{r_d}$$
$$h_{abs} = H_v - h_s + x_s \left.\frac{\partial h_s}{\partial x_s}\right|_{T_s} \tag{4}$$

The interphase conditions are evaluated assuming that the temperature at the interphase is equal to the newly formed film temperature. The time for drop formation is calculated as:

$$t_{\text{form}} = \frac{m_d N}{\Gamma_s} \tag{5}$$

3.4. Droplet fall regime

This regime occurs in the trajectory of the lower part of a refrigerant pipe to the upper part of the next pipe, since the drop keeps forming until this drop touches the surface of the next pipe.

In the free falling drop regime, the mass and energy equations are the result of balances applied to a falling drop [1].

Mass balance:

$$\frac{\mathrm{d}m_d}{\mathrm{d}t} = 4K_{\mathrm{fall}}\,\rho\pi R^2 \frac{(x_s - x_i)}{100} \quad (6)$$

Energy balance:

$$m_d Cp_s \frac{\mathrm{d}T_s}{\mathrm{d}t} = h_{abs}\frac{\mathrm{d}m_d}{\mathrm{d}t} \quad (7)$$

The temperature at the interphase is calculated as:

$$T_i = \frac{h_{abs}}{16\pi k R}\frac{\mathrm{d}m_d}{\mathrm{d}t} + T_s \quad (8)$$

The interphase composition is obtained by Eq. (1). The time for free falling drop is evaluated with a simple droplet fall expression

$$t_{fall} = \sqrt{\frac{2S}{g}} \quad (9)$$

3.5. Falling film regime (Fig. 4)

In the falling film regime, the mass and energy equations are the result of the balances applied to a fine film in a horizontal pipe [1].

Mass balance in the absorbent mixture

$$\frac{\mathrm{d}w_s}{\mathrm{d}\theta} = K_{film}\rho(r_\circ + \delta)\frac{(x_s - x_i)}{100} \quad (10)$$

Energy balance in the absorbent mixture

$$w_s \left.\frac{\partial h}{\partial T_s}\right|_x \frac{\partial T_s}{\partial\theta} = \left[\left(h_{abs} - h_s + x_s \left.\frac{\partial h}{\partial x}\right|_T\right)\frac{\partial w_s}{\partial\theta} - Ur_\circ (T_s - T_c)\right] \quad (11)$$

Energy transfer in the refrigerant fluid

$$w_c Cp_c \frac{\mathrm{d}T_c}{\mathrm{d}z} = U(\bar{T}_s - T_c) \quad (12)$$

The temperature at the interphase in this regime is calculated as:

$$T_i = \frac{1}{4}\frac{h_{abs}}{k}\frac{\delta}{(r_\circ + \delta)}\frac{\mathrm{d}w_s}{\mathrm{d}\theta} + T_s \quad (13)$$

Composition at the interphase is obtained by Eq. (1). The residence time for the falling film regime is evaluated based on the average film speed ($\bar{u}$), and the film thickness (δ), assuming laminar flow:

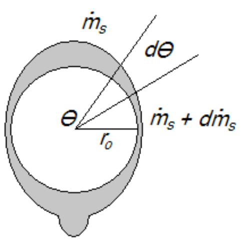

Fig. 4. Falling film regime.

$$t_{film} = \int_0^{\pi}\frac{r_o}{\bar{u}}\mathrm{d}\theta \quad (14)$$

Average speed and film thickness are evaluated as:

$$\bar{u} = \frac{\Gamma_s}{2\delta\rho} \quad (15)$$

$$\delta = \left(\frac{3\mu\Gamma_s}{\rho^2 g \sin\theta}\right)^{\frac{1}{3}} \quad (16)$$

3.6. Mass and energy transfer coefficients

To evaluate the heat transfer coefficient of the absorbent mixture and the refrigerant flow (λ_s and λ_c), we use the correlations proposed by Kay and Nedderman [12], which depend on Nusselt number. To calculate the diffusion coefficient we use the relationship proposed by Wike-Chang [13]:

$$D_{AB} = 7.4\times10^{-8}\frac{\sqrt{\psi_B M_B}\,T}{\mu_B \bar{V}_A^{\,0.6}} \quad (17)$$

Global heat transfer is calculated by the following relationship.

$$\frac{1}{U} = \frac{r_o}{r_i\lambda_c} + \frac{r_o \ln\left(\frac{r_o}{r_i}\right)}{k_w} + \frac{1}{\lambda_s} \quad (18)$$

In this equation, it is observed that the terms of the energy transfer from the absorbent mixture, which flows from the falling film to the refrigerant flow, has these mechanisms: (i) convection from the film to the pipe (ii) conduction through the walls of the pipe and (iii) convection from the wall of the refrigerant pipe to the refrigerant flow.

The mass transfer coefficients are given by empirical relations [11]. They are summarized in Table 3 at the operating conditions given by Table 2.

Table 2
Operating conditions

Operating conditions	Values
Input concentrated mixture	4.43 e–3 kg/s, 81.1°C, 56%, 300–330 mmHg
Output diluted mixture	4.04 e–3 kg/s , 94.6°C, 54%
Input feed steam from evaporator	79.7°C
Input water	3.0167 e–03 l/s, 91.06°C
Output evaporated water	93.65°C

Table 3
Mass transfer and residence time of every regime

Regime	Mass transfer equation (average value)	Average residence time
Drop formation [14]	$K_{\text{form}} = \frac{24}{7}\sqrt{\frac{D}{\pi t_{\text{form}}}}$	$t_{\text{form}} = \frac{m_d N}{\Gamma_s}$ (= 0.76 s)
Droplet fall	$K_{\text{fall}} = 35\frac{D}{2R}$	$t_{\text{fall}} = \sqrt{\frac{2S}{g}}$ (= 0.032 s)
Falling film	$K_{\text{film}} = \frac{D}{\delta}$	$t_{\text{film}} = \int_0^{\pi} \frac{r_o}{u} d\theta$ (= 1.85 s)

From Table 3 we see that the droplet fall regime is very small. The falling film regime is more than two times the value of drop formation.

3.7. Numerical solution

The evaluation of properties at the interphase conditions T_i,x_i, for instance Eqs. (1), (8) were solved analytically to reduce nested iterations. The ordinary differential equations, which model the two-dimension behavior of the absorber, were solved by the Runge–Kutta method. The configuration of pipes requires an iterative convergence which was achieved by the over-relaxation method. The computer code was developed using the Matlab ® computer language. Also, a profiler provided in this language was used to identify blocks of code which could be programmed more efficiently.

4. Results and discussion

The input flow and the output temperature of the absorber were obtained experimentally from the reference equipment at CIICAp (Fig. 5). The analysis of its effect is discussed in the next sections.

4.1. Effect of every regime

The plot of temperature vs. residence time shows that as the LiBr-H_2O descends along the vertical pipes, the mixture becomes hotter (Fig. 6). During falling film regime, due to the value of the temperature gradient, the LiBr-H_2O mixture transfers heat to the water. During the drop formation regime, as the mixture arrives to the bottom of the pipe, there is a limited heat transfer of the drops to the water, thus the overall effect of heat transfer and heat of absorption is heating. As the mixture descends, it becomes warmer, so it can transfer more heat to the water. The overall effect in the temperature of mixture is a saw teeth profile shown in Fig. 6.

The residence time of droplet fall regime is very small; as a result, this regime has a small contribution in the heat and mass transfer. Falling film regime has the largest residence time, and during this regime, the heat is transferred to the water to evaporate. During drop formation regime, the mixture is heated.

4.2. Effect of configuration of the pipes

The configuration of the pipes allow the hottest temperature in pipes 2 and 3. This configuration promotes the evaporation of water to be purified. As the mixture travels from upper 1–2 to lower pipes 3–4, the absorption heat released is smaller; thus, in the pipes 4, the final dynamics of heat released and heat transferred is that the mixture becomes cooler. If the mixture enters at a higher

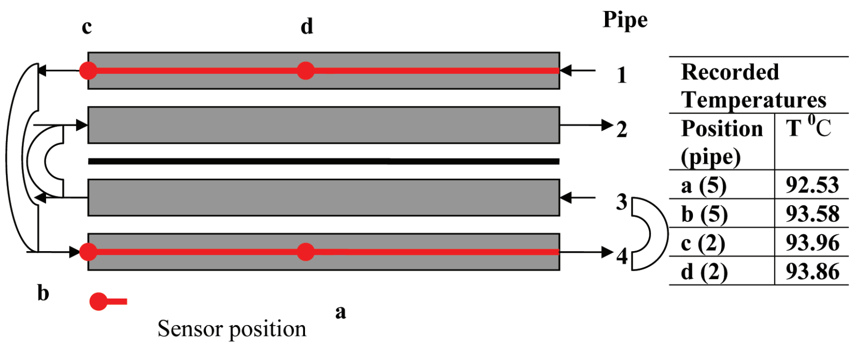

Fig. 5. Sensor positions in the absorber.

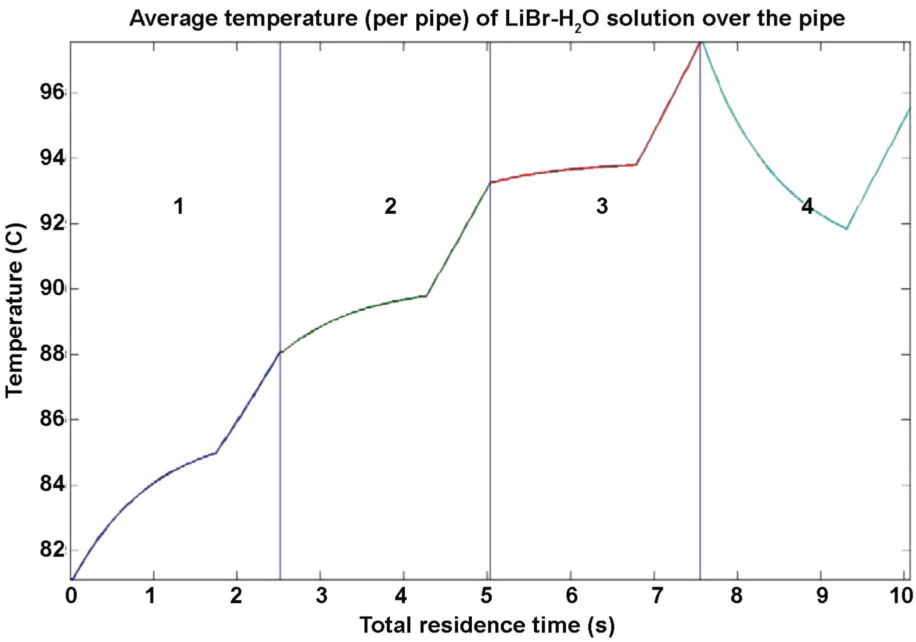

Fig. 6. Mixture temperature vs. residence time.

temperature, the pressure in the shell side increases. This increase makes the absorption process more difficult.

4.3. Effect on water to be purified

The water to be purified enters at conditions near to saturation in pipe 1, and then it travels to pipe 4 where the mixture is near the saturation conditions. Then the water travels to pipes 3 and 2. These pipes are used to fully evaporate the water (see Fig. 7), since the steam produced in these pipes exchanges energy with a hot mixture of LiBr-H_2O.

5. Conclusions

With this dynamic model, it is possible to appreciate the heat profiles along the absorber. The changes of properties in this horizontal absorber are narrow (3% compo-

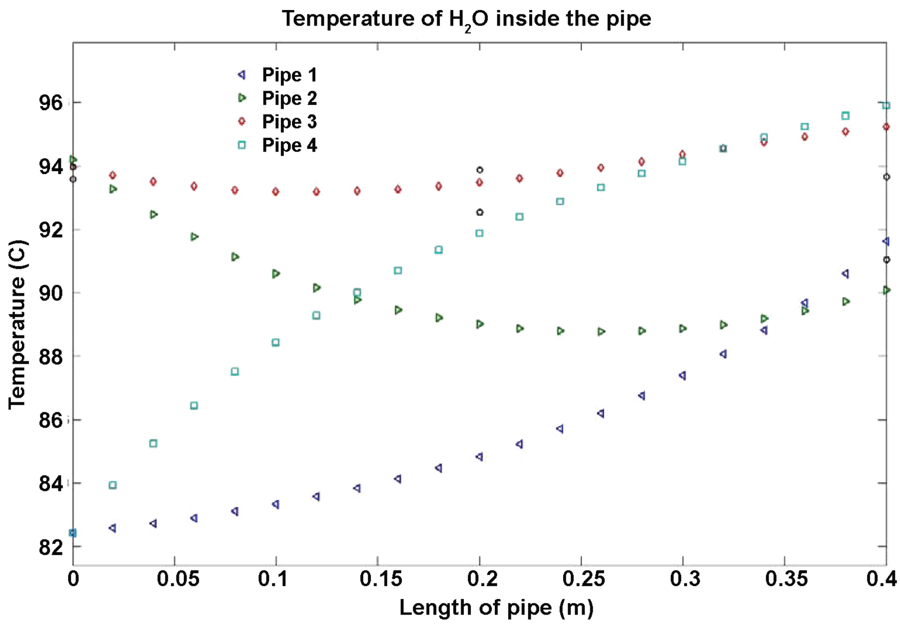

Fig. 7. Temperature of H_2O vs. pipe length. 'o' indicates experimental data.

sition, 14°C for mixture, and 2°C, overall, for water to be purified), thus, a comparison with a global model offers little improvement in accuracy. However, this model is useful to predict hot spots, which at the same time point out ways to improve operating and the feed conditions. It has also been observed that the performance of the absorber is very sensitive to the operating pressure. In particular, as a future work is to increase the temperature of LiBr-H_2O mixture to obtain a higher heat transfer.

Also an improvement has been achieved by a recycling heat to the generator.

Symbols

COP — Coefficient of performance = QAB/(QGE + GEV)
Cp — Specific heat, kJ/kg K
D — Mass diffusivity, m^2/s
g — Gravitational acceleration, m/s^2
H — Enthalpy of water vapour, kJ/kg
h — Enthalpy of liquid, kJ/kg
h_{abs} — Absorption heat, kJ/kg
k — Thermal conductivity, kW/m K
K — Mass transfer coefficient, m/s
M — Molecular weight, g/gmol
m — Mass, kg
N — Number of dripping sites per pipe length, m^{-1}
P — Pressure, mmHg
Q — Heat flow, kW/m^2 K
r — Radius of the pipe for the refrigerant fluid, m
R — Drop radious, m
S — Spacing between tubes, m
t — Time, s
T — Temperature, ºC
u — Velocity of decendant film, m/s
U — Overall heat transfer coefficient, kW/m^2 K
V — Molar volume, cm^3/gmol
W, w — Mass flow, kg/s
x — LiBr mass fraction, %
z — Horizontal coordinate of the absorber, m

Greek

Γ — Mass flow per unit length of pipe = W/2 L, kg/m s
δ — Descendent film width, m
θ — Angular coordinate, rad
λ — Thermal conductivity, W/m K
μ — Dynamic viscosity, kg/m s
ϱ — Density, kg/m^3
σ — Film thickness, N/m
ψ — Association parameter

Subscripts

A — LiBr
B — Water
AB — Absorber
b — Bulk
c — Refrigerant flow
d — Drop
form — Formation regime
fall — Free falling regime
film — Descententent flow regime
i — Interface, inlet
o — Outer
s, sol — Mixture
v, vp — Vapor
w — Wall
WF — Working fluid

References

[1] M.J. Kirby and H. Pérez-Blanco, A design model for horizontal tube water/lithium bromide absorbers, Heat Pump Refrig. Syst. Design, 32 (1994) 1–10.
[2] M.D. Determan, Experimental and analytical investigation of ammonia–water desorption in microchannel geometries, M.Sc. Mech Eng. thesis, Georgia Inst. of Technology, 2005.
[3] J.D. Killion and S. Garimella, Pendant droplet motion for absorption on horizontal tube banks, Int. J. Heat Mass Transfer, 47 (2004) 4403–4414.
[4] I. Kyung, K.E. Herold and Y.T. Kang, Experimental verification of H_2O/LiBr absorber bundle performance with smooth horizontal tubes, Intl. J. Refrig., 30 (2007) 582–590.
[5] I. Kyung, K.E. Herold and Y.T. Kang, Model for absorption of water vapour into aqueous LiBr flowing over a horizontal smooth tube, Intl. J. Refrig., 30 (2007) 591–600.
[6] F.A. Holland, J. Siqueiros, S. Santoyo, C.L. Heard and E.R. Santoyo, Water Purification Using Heat Pumps, E. and F.N. Spon/Routledge, London–New York, 1999.
[7] A. Huicochea, Startup and experimental evualuation of a portable water purification system integrated to a heat transformer, MSc thesis, Cenidet, 2004.
[8] J. Torres-Merino, Contacteurs gaz-liquide pour pompes a chaleur a absorption multi-stagees, PhD thesis, Institut National Polytechnique de Lorraine, France, 1997.
[9] L.A. McNeely, Thermodynamics properties of aqueous solution of lithium–bromide, ASHRAE, 85 (1979) 413–434.
[10] B.E. Poling, J.M. Prausnitz and J.P. O'Conell, The Properties of Gases and Liquids, 5th ed., McGrawHill, 2000.
[11] S. Jeong and S. Garimella, Falling-film and droplet mode heat and mass transfer in a horizontal tube LiBr/water absorber, Int. J. Heat Mass Transfer, 45(7) (2002) 1445–1458.
[12] J.M. Kay and R.M. Nedderman, Fluid Mechanics and Heat Transfer, Cambridge University Press, London–New York–Melbourne, 1974, pp. 120–121.
[13] R.B. Bird, W.E. Stewart and E.N. Lightfoot, Transport Phenomena, 2nd ed., OUP, 2001.
[14] R. Clift, J. Grace and M.E. Weber, Bubbles, Drops, and Particles, Dover Pub. Inc., 1978.